

The SPICA coronagraphic instrument (SCI) for the study of exoplanets

K. Enya,^{a,*} T. Kotani,^a K. Haze,^{b,a} K. Aono,^{c,a} T. Nakagawa,^a
H. Matsuhara,^a H. Kataza,^a T. Wada,^a M. Kawada,^a
K. Fujiwara,^a M. Mita,^a S. Takeuchi,^a K. Komatsu,^a S. Sakai,^a
H. Uchida,^d S. Mitani,^d T. Yamawaki,^d T. Miyata,^e S. Sako,^e
T. Nakamura,^e K. Asano,^e T. Yamashita,^f N. Narita,^f
T. Matsuo,^f M. Tamura,^f J. Nishikawa,^f E. Kokubo,^f
Y. Hayano,^g S. Oya,^g M. Fukagawa,^h H. Shibai,^h N. Baba,ⁱ
N. Murakami,ⁱ Y. Itoh,^j M. Honda,^k B. Okamoto,^l S. Ida,^m
M. Takami,ⁿ L. Abe,^o O. Guyon,^p P. Bierden,^q T. Yamamuro^r

^a*Institute of Space and Astronautical Science, Japan Aerospace Exploration
Agency,
3-1-1 Yoshinodai, Chuo-ku, Sagamihara, Kanagawa 252-5210, Japan*

^b*The Graduate University for Advanced Studies, 3-1-1 Yoshinodai, Sagamihara,
Tyuou-ku, Kanagawa 252-5210, Japan*

^c*Department of Physics, Graduate School of Science, University of Tokyo,
Bunkyo-ku, Tokyo 113-0033, Japan*

^d*Aerospace Research and Development Directorate, Japan Aerospace Exploration
Agency, Tsukuba Spcae Center, 2-1-1 Sengen, Tsukuba-shi, Ibaraki 305-8505,
Japan*

^e*Institute of Astronomy, School of Science, University of Tokyo, 2-21-1 Osawa,
Mitaka, Tokyo 181-0015, Japan*

^f*National Astronomical Observatory of Japan, 2-21-1 Osawa, Mitaka, Tokyo
181-8588, Japan*

^g*Subaru Telescope, National Astronomical Observatory of Japan, 650 North
A'ohoku Place, Hilo, Hawaii 96720, U.S.A.*

^h*Department of Earth and Space Science, Graduate School of Science, Osaka
University, 1-1 Machikaneyama, Toyonaka, Osaka 560-0043, Japan*

ⁱ*Division of Applied Physics, Faculty of Engineering, Hokkaido University,
Sapporo 060-8628, Japan*

^j*Graduate School of Science and Technology, Kobe University, 1-1 Rokkodai,
Nada, Kobe 657-8501, Japan*

^k*Department of Information Sciences, Kanagawa University, 2946 Tsuchiya,
Hiratsuka, Kanagawa, 259-1293, Japan*

^l*Institute of Astrophysics and Planetary Sciences, Faculty of Science, Ibaraki*

University, 2-1-1 Bunkyo,Mito, Ibaraki 310-8512, Japan

^m*Tokyo Institute of Technology, Ookayama, Meguro-ku, Tokyo 152-8551, Japan*

ⁿ*Institute of Astronomy and Astrophysics, Academia Sinica. P.O. Box 23-141,
Taipei 10617, Taiwan, R.O.C*

^o*Laboratoire Fizeau, Université de Nice Sophia-Antipolis, Parc Valrose, 06108
Nice Cedex 02, France*

^p*Subaru Telescope, National Astronomical Observatory of Japan, 650 North
A'ohoku Place, Hilo, Hawaii96720, U.S.A.*

^q*Boston Micromachines Corporation, 30 Spinelli Place, Cambridge, MA 02138,
U.S.A*

^r*Optcraft Corporation, 3-16-8 Higashi-Hashimoto, Sagamihara, Midori-ku,
Kanagawa 252-0144, Japan*

Abstract

We present the SPICA Coronagraphic Instrument (SCI), which has been designed for a concentrated study of extra-solar planets (exoplanets). SPICA mission provides us with a unique opportunity to make high contrast observations because of its large telescope aperture, the simple pupil shape, and the capability for making infrared observations from space. The primary objectives for the SCI are the direct coronagraphic detection and spectroscopy of Jovian exoplanets in infrared, while the monitoring of transiting planets is another important target. The specification and an overview of the design of the instrument are shown. In the SCI, coronagraphic and non-coronagraphic modes are applicable for both an imaging and a spectroscopy. The core wavelength range and the goal contrast of the coronagraphic mode are 3.5–27 μ m, and 10^{-6} , respectively. Two complementary designs of binary shaped pupil mask coronagraph are presented. The SCI has capability of simultaneous observations of one target using two channels, a short channel with an InSb detector and a long wavelength channel with a Si:As detector. We also give a report on the current progress in the development of key technologies for the SCI.

Key words:

SPICA, coronagraph, instrument, SCI, exoplanet, infrared

* Corresponding author.

Email address: enya@ir.isas.jaxa.jp (K. Enya)

1 Background and Scientific Objective

We regard the systematic study of extra-solar planets (exoplanets) to be one of the most important tasks to be undertaken in space science in the near future. The enormous contrast between the parent star and the planet presents us with a serious problem. Therefore, there is a requirement for special instruments using techniques specifically designed to improve the contrast in order to perform a systematic observation of exoplanets. There are a number of different techniques currently used to observe exoplanets. Since the first report by Mayor & Queloz (1995) using the radial velocity method, more than 450 exoplanets have been discovered. It has also been shown that observations monitoring the transits of exoplanets provide a valuable means for studying them (Charbonneau et al., 2000). Not only detection but also spectroscopic studies of some transiting exoplanets have been carried out (e.g., Deming et al. (2005); Tinetti et al. (2007); Swain et al. (2010)). Recently, the spatially resolved direct detection of an exoplanet by coronagraphic imaging was finally reported (e.g., Marois et al. (2008); Kalas et al. (2008)). While these methods are quite valuable, the current targets of these methods tend to be strongly biased. Many of the targets for radial velocity observations and the monitoring of transiting planets are Hot-Jupiters that are close to their parent stars. On the other hand, exoplanets observed by current coronagraphic imaging tend to be strongly limited to young, giant outer planets. So the coronagraphic observation of mature, outer planets is still missing from the population. Considering this situation, we believe that the next important step in this field is a systematic study of exoplanets of various ages, masses, and distances from their parent stars. A spectroscopic survey of known exoplanets is especially important for characterizing planetary atmospheres.

The Space Infrared telescope for Cosmology and Astrophysics (SPICA) is an astronomical mission optimized for mid-infrared (MIR) and far-infrared astronomy with a 3m class (~ 3.0 m effective pupil diameter/ ~ 3.2 m physical diameter in the current design) on-axis telescope cooled to < 6 K (Nakagawa et al., 2010). We have proposed to develop a Coronagraphic Instrument for SPICA (SCI) and to carry out essential study in exoplanet science with the SCI (P.I.: K. Enya; Enya et al. (2010) and its references).

SPICA has advantages as the platform for the SCI: it is perfectly free from band pass limitations and wavefront turbulence caused by the atmosphere. The cryogenic telescope provides high sensitivity in the infrared region. High stability is expected as the cryogenic telescope is to be launched into deep space, the Sun-Earth L2 Halo orbit. In addition, the structure of the SPICA telescope, adopting a monolithic primary mirror and carefully designed secondary support, yields a clean point spread function (PSF).

The major scientific tasks are described below. We regard that the instrument should be designed to carry out two “critical tasks”; one is the coronagraphic detection and characterization of exoplanets, and, the other is the monitoring of transiting planets. There are other important scientific tasks which can be carried out with the “given” performance of the designed instrument.

(1) Coronagraphic observations:

One of the two critical scientific tasks for the SCI is to pursue the direct detection and spectroscopy of exoplanets. The SCI suppresses light from the parent star, and in spectroscopy mode working with coronagraph reveals essentially important spectral features in the MIR region, CH₄, H₂O, CO₂, CO, NH₃. Jovian exoplanets around (1) nearby stars ($\leq 10\text{pc}$) and (2) young and moderately old stars ($\leq 1\text{Gyr}$ old) are the primary targets for coronagraphic observations with the SCI (Fig.1). The former are suitable for detailed spatially-resolved observations, and the latter for gaining an understanding of the history of the formation of the planetary system. With the SCI we expect to be able to create an atlas of the various spectra of exoplanets by making observations on $\sim 100\text{s}$ of targets. More detail is given in Fukagawa, Itoh, & Enya (2009), Matsuo et al. (2011).

(2) Monitoring transiting planets:

The other critical scientific task is precise monitoring of transiting planets in order to characterize their spectral features. Coronagraphic observations by the SCI cover the “outer planets”, i.e., those at $\sim 10\text{AU}$ or further from the parent star. Therefore, the observation of transiting planets and coronagraphic observations are complementary techniques. It should be noted that the method for monitoring transiting planets requires the planets to be in edge-on orbits, and therefore discovery before observation with SPICA. The SCI has many advantages as a transit monitoring instrument. It has the capability for simultaneous observations with two detectors, having filters optimized for the spectral features of planetary atmospheres. Of the focal plane instruments on the SPICA mission, only the SCI covers the spectrum down to wavelengths of $\sim 1\mu\text{m}$ (coronagraphic high contrast images are guaranteed only for wavelengths down to $3.5\mu\text{m}$; however the instrument has an InSb detector which is sensitive at shorter wavelengths). Another advantages of the SCI for this task are the superior pointing stability in the SPICA instruments, 0.05arcsec can be realized by an internal sensor, and potential capability for defocusing to avoid saturation by using an internal deformable mirror. Additionally, partial readout of the detectors can be adopted to improve the exposure/readout duty cycle when imaging.

(3) Other observations of planetary systems:

Some other important observations relating to extra-solar planetary sys-

tems are planned with the given instrument design. Color Differential Astrometry (CDA) is being considered for the observation of planetary systems (Abe et al., 2009). CDA is a challenging method, but it has the advantage of having the capability of observing “inner planets” and does not require planets in edge-on orbits. Observations of the “snow line” (e.g., Honda et al. (2009)) and other features in circumstellar disks are other important targets for the SCI (Tamura et al. (2009); Takami et al. (2010)).

By using the spectral data sets of various exoplanets obtained by the SCI, we expect that our understanding of the whole planetary system will be significantly improved.

2 Instrument

2.1 Specification

The specification of the instrument is summarized in Table 1. An overview of the current optical design of the SCI is shown in Fig.2. The requirement that gives us the limiting short wavelength ($3.5\mu\text{m}$) is derived for the direct detection and spectroscopy of Jovian exoplanets. As shown in Fig. 1, it is expected that the Spectral Energy Distribution (SED) of Jovian exoplanets has a peak in the $3.5\text{--}5\mu\text{m}$ wavelength region (Burrows2003). So this wavelength region is one of the most appropriate regions for the direct detection of Jovian planets. Wavelength coverage from MIR to $3.5\mu\text{m}$ allows us to study interesting molecular features of the planetary atmospheres, e.g., H_2O , CH_4 , NH_3 . The goal contrast (10^{-6} at PSF) is derived for the systematic study of Jovian planets, including not only extremely massive, young planets but lower mass planets (down to $\sim 1M_J$ with 1Gyr old targets) and older planets (up to 5Gyr old massive targets). It should be noted that the PSF subtraction technique has the potential to improve the final contrast after image processing, e.g., by one order or more (Trauger & Traub (2007); Haze et al. (2009)). Although the diffraction limited image at a wavelength of $5\mu\text{m}$ is a specification of the SPCIA telescope, wavefront correction using a deformable mirror (DM), make observations at shorter wavelengths possible with the SCI. The SCI is primarily used for coronagraphic imaging and in coronagraphic spectroscopy mode. On the other hand, non-coronagraphic imaging and spectroscopy are also possible because the coronagraph mask can be removed. In non-coronagraphic mode the SCI is useful as a general purpose fine-pixel camera and a spectrometer.

The high contrast in the coronagraphic image is guaranteed only within a field determined by the inner working angle (IWA), the outer working angle (OWA), and the number of actuators in the DM, whereas the SCI has a FoV of $1' \times 1'$. The number of DM actuators is 32×32 which provides the capability to control the wavefront over an area of $16\lambda/D \times 16\lambda/D$ in the coronagraphic image. This high contrast area, $16\lambda/D \times 16\lambda/D$, determines the limit to the outer working angle (OWA) in the design of the coronagraph shown in Table. 1.

Two channels, a short and a long wavelength channel, have been adopted, together with a beam splitter. The short and long wavelength channels have an InSb and a Si:As detector, respectively, and cover the wavelength regions $\leq 5\mu\text{m}$ and $\geq 5\mu\text{m}$. This two channel design has some advantages: First, a higher sensitivity for the $3.5\text{--}27\mu\text{m}$ wavelength region is obtained compared to a single channel design. Secondary, the simultaneous observation of one target with two channels is possible. Thirdly, an appropriate pixel scale can be determined for each channel. In the current design, $1.5 \times$ Nyquist sampling (i.e., over sampling) at $3.5\mu\text{m}$ and $5\mu\text{m}$ has been adopted for the short and long channels, respectively. The simultaneous observation of one target with two channels is possible.

The IWA of the SCI, $3.3\lambda/D$, corresponds to ~ 1 and ~ 2 arcsec at wavelengths of $5\mu\text{m}$ and $10\mu\text{m}$, respectively. These values are no smaller than those of the next generation of ground based coronagraphs, e.g., the Gemini Planet Imager (GPI) or coronagraphs for 30m class telescopes. However, such coronagraphs used with ground based telescopes mainly work only in the window of atmospheric transmittance in infrared. This suggests that ground based coronagraphs are useful for imaging young planets, and are complementary to the SCI's capability for wide band spectroscopy for cooler exoplanets. In comparison with the JWST coronagraphs, the most important advantage of the SCI is its capability for spectroscopic measurements which JWST does not have. Furthermore, the contrast of the SCI is significantly higher owing to the active wavefront control. The capability of the simultaneous use of two channels in the SCI is useful for image subtraction of coronagraphic observations, and monitoring transiting planets with wide wavelength coverage, which is not possible with JWST. Matsuo et al. (2011) presents more on the comparison between the SCI and the JWST coronagraphs, especially on the point of detectability of outer cooled planets.

2.2 Overview of the Instrument

The optics of the SCI is compact with the optical axis in one plane (Fig. 2). The total mass is $\sim 30\text{kg}$ and the whole instrument, together with the telescope, is cooled to 5K before operation to enable the SPICA to achieve ultra-

high sensitivity in the far- and mid-infrared regions. The SCI uses the center of the field of view in the focal plane of the telescope to obtain the best wavefront accuracy and symmetry of the obscuration by the secondary mirror and its support structure (Fig. 3). All the mirrors for collimation and focusing in the SCI are off-axis parabolas. Aberration is minimized at the center of the FoV in order to obtain the best coronagraphic PSF of the parent star. The pre-coronagraphic optics and the coronagraphic optics are common for both wavelength channels, while the post-coronagraphic optics is split into two channels.

The pre-coronagraphic optics consists of reflective optical devices in order to avoid ghosts and/or a wavelength dependent refractive indices which are sometimes issues in lens optics. In contrast to the other focal plane instruments on the SPICA mission, the SCI has no pick-off mirror, with the beam from the telescope secondary mirror arriving directly on the collimating mirror (Fig. 2). This configuration makes the SCI compact under the constraint presupposing no lens optics. Minimizing the number of mirrors reduces the total light scattering at the surfaces of the mirrors. The first mirror of the SCI is placed after the focal point of the telescope. This is convenient for optically testing the SCI and the telescope. A DM is included in the SCI to correct the wavefront errors of the telescope.

As shown in Fig. 4, the baseline solution for the coronagraphic method is a binary-shaped pupil mask (see Sec. 3.1). With this method, only one pupil mask modifies the PSF and provides the required contrast. A focal plane mask is used to obscure the bright core in the coronagraphic PSF and to prevent scattered light from the PSF core polluting the dark region of the coronagraphic PSF in the post-coronagraphic optics. Interchangeable focal plane masks will be used to realize different observing modes, including a slit that can be used both with and without the pupil mask to provide spectroscopic capability in coronagraphic and non-coronagraphic observing modes. Fig. 5 shows the concept of spectroscopy working together with coronagraphy in the SCI.

The post-coronagraphic optics uses a beam splitter to split the optical path into two channels, the short wavelength channel with an InSb detector and the long wavelength channel with a Si:As detector. Each channel has filter wheels, and simultaneous observation of the same target with the two channels is possible. Each filter wheel contains a transmissive disperser (e.g., a grism) for spectroscopy.

In order to reduce technical risk in the development, another design of the instrument without the use of a DM is also under consideration, together with the full-equipped solution described above. As the result of this simplification, the contrast at the PSF is limited to be $\sim 10^{-4}$. In this case, the

advantage of high contrast over JWST is basically lost. However, the spectroscopy working with coronagraph remain a unique capability of the SCI. It is already known that there are young outer planets observed by direct imaging (e.g., Marois et al. (2008)). These planets are enough bright in infrared for the spectroscopic observation using the simplified design of the SCI. We believe that the spectrum data of such targets for the wide infrared wavelength range is essentially unique and important.

3 Key technologies

The SCI requires challenging technologies to realize high contrast for both imaging and spectroscopy over a wide MIR wavelength range. One of the critical technologies is the design, development and manufacture a coronagraph which can yield a high contrast PSF. We focused on a coronagraph using a multiple 1-dimensional barcode mask (Enya & Abe, 2010) which is a type of binary shaped pupil mask (e.g., Kasdin et al. (2005); Vanderbei, Kasdin, & Spergel (2004); Tanaka et al. (2006)). Another key technology is the adaptive optics, which improves the wavefront and stability of the PSF because the specification for these is more critical for the SCI than for the SPICA. Optical ghosts and scattering in the SCI should be enough nullified practically to avoid polluting the high contrast image. With this in mind, the development of a cryogenic MIR chamber for end-to-end tests of the coronagraph are ongoing. More details are presented in the following sections.

3.1 Coronagraph

A coronagraph to produce high contrast images is the core function of the SCI. The coronagraph for SPICA has to work over a wide MIR wavelength region in a cryogenic environment, so a coronagraph without transmissive optical devices is preferable. The coronagraph should be insensitive to telescope pointing errors caused by vibration from the cryogenic cooling system and the attitude control system. Achromatism (except the scaling effect for the size of the PSF) is also an important property. The coronagraph should be applicable for the pupil of the SPICA, which is partly obscured by the secondary mirror and its support structure. After taking these points into consideration, a coronagraph using a binary shaped pupil mask was selected as the primary method for our study. Experiments were carried out to confirm the feasibility of this strategy.

- Demonstration of the principle:

First we carried out experiments to validate the performance of the coron-

agraph with a checkerboard mask, which is a type of binary shaped pupil mask, using a visible laser in an air ambient. Checkerboard masks consisting of 100nm thick aluminum patterns on BK7 glass substrates were constructed using nano-fabrication technology. Electron beam lithography and a lift-off process were used in the fabrication process. Optimization of the checkerboard masks was executed using the LOCO software presented by Vanderbei (1999). The contrast, derived by averaging over the dark region using a linear scale and comparing this with the peak intensity, was 6.7×10^{-8} (Fig. 6-(c),(d)).

- Multi-band experiment with non-zero bandwidth light sources:

We installed multi-band Super Luminescent Diode Light Sources (SLED) for this experiment, and confirmed that the binary shaped pupil mask coronagraph works for light sources with center wavelengths (λ) of 650, 750, 800, 850nm with bandwidths ($\Delta\lambda$) of 8, 21, 25, and 55nm, respectively. The results of this experiment are shown in Fig. 7. More details are given in Haze et al. (2010).

- Mask design for the SPICA pupil:

We designed some binary shaped pupil masks for the SPICA pupil mask having the obscuration shown in Fig. 4. These designs consist of multi-barcode masks and have coronagraphic power in one dimension only. As a result, large opening angle is realized with keeping to satisfy the specification for the IWA. In the masks shown in Fig. 4, mask-1 is the baseline design. Additionally, mask-2 provides a small IWA to explore the field closer to the parent star. On the other hand, the contrast of mask-2 is not as high as mask-1 because there is a trade-off between the IWA and the contrast. These two masks are complementary, and can be changed by a mechanical mask changer. It should be noted that the principle of the barcode mask was presented by Kasdin et al. (2005). More details are presented in Enya & Abe (2010)

- Free standing masks:

The trial fabrication of free standing masks (i.e., masks without a substrate) was carried out using various manufacturing methods. We tested the coronagraphic performance using a manufactured free standing mask made of thin copper plate and a visible He-Ne laser (Fig. 8). This mask was also used in an experiment to demonstrate wavefront correction, and this was found to work successfully with this mask (see Sec. 3.3).

Combining these results implies that it is reasonable to assume that our binary shaped pupil mask coronagraph will work at MIR wavelengths. The development of a cryogenic chamber for end-to-end demonstration of the MIR coronagraph is ongoing (see Sec. 3.4). Toughness tests with vibration and acoustic

load is to be undertaken for the mask in future work.

3.2 Adaptive optics

The specification for the wavefront quality of the SPICA telescope is 350 nm rms, while the requirement for the SCI is higher by a factor of 10 or more. Therefore, the SCI needs an internal active wavefront correction system which works at the temperature of the SCI (i.e., 5K). Therefore, we began the development of a cryogenic DM, which is one of the critical components needed to realize the SCI.

- Demonstration with a prototype device:

We developed a prototype DM with 32 channels consisting of a Micro Electro Mechanical Systems (MEMS) chip fabricated by the Boston Micromachines Corporation (BMC) and a special silicon substrate designed to minimize the thermal stress caused by cooling. Fig.9 shows the result of a demonstration with this prototype in a cryogenic environment. For the first step of this work, a liquid nitrogen cooled chamber was used (i.e., without liquid helium) for convenience. As a result, the lowest temperature of the DM was limited to 95K. More than 80% of the linear thermal shrinkage of the silicon when cooling from room temperature to 5K occurs in the temperature range from 293 to 95K (Okaji & Yamada , 1999). This fact suggests that the development strategy starting is reasonable. For the full demonstration of the cryogenic DM, development of a cryogenic 32×32 channel DM and a 5K chamber is ongoing. More details are given in Enya, Kataza, & Bierden (2009).

- Structural analysis of a 1000 channel DM:

From the studies with the prototype, we found that the thermal stress is the critical issue for our cryogenic DM if we intend to go to a larger format, e.g., a 1000 channel DM. Therefore, we carried out simulation studies of the thermal deformation and stress induced by cooling in order to obtain design solutions that would maintain the flatness of a 1000 channel DM cooled to 5K. We obtained an initial design, and further improvement is ongoing.

- Development of a film print cable:

Parasitic heat passing through the cables between the cooled DM and the warm electronics is another important issue. In the SPICA mission, the allocated parasitic heat for all focal plane instruments is limited to only 10mW. We attempted the manufacture of film print cables in order to reduce the parasitic heat to an ultra-low level (<1mW via 1000 cables). We confirmed that the first version of our film print cable is sufficiently thin and provides

electrical insulation up to 200V (Fig. 9).

These results suggest that the development of a cryogenic DM with 1000 channels is viable and that it will work at 5K. We are also considering a cryogenic multiplexer as a backup solution to the film print cables. Testing of toughness of the cryogenic DM will be also undertaken in future work.

3.3 *Wavefront correction*

Another important issue is how to operate a DM in order to correct wavefront errors. To develop an algorithm for SPICA/SCI, we initiated experiments using a visible laser, a commercially-available DM from BMC, a free standing coronagraph mask having the checkerboard design, and a CCD camera. Coronagraphic images were taken, and the speckle nulling method was applied to cancel the speckle in a dark region of the PSF (Malbet, Yu, & Shao, 1995). A remarkable improvement of the coronagraphic contrast, to become much better than 10^{-6} , was confirmed for an area just outside the inner working angle, which is an important area in the search for exoplanets (Fig. 10). The algorithm used in this experiment included hundreds of iterations to produce anti-speckles. We plan in future work to try a more sophisticated algorithm which requires less number of images with different phases as presented in Bordé, & Traub (2006), Give'on et al. (2007). For the SCI, the phase shift will be achieved by operating an internal device (i.e., a deformable mirror) or moving the secondary mirror of the SPICA telescope. More detail is given in Kotani et al. (2010).

3.4 *Cryogenic MIR Testbed*

Our previous laboratory experiments on the coronagraph were performed at room temperature and atmospheric pressure, and at visible wavelengths, whereas the SPICA coronagraph will have to be evaluated at cryogenic temperatures, in a vacuum, and at infrared wavelengths. In order to complete end-to-end testing of the MIR coronagraph at 5K, we are developing a cryogenic vacuum chamber in the Institute of Space and Astronautical Science (ISAS) of the Japan Aerospace Exploration Agency (JAXA). The cryogenic DM and free-standing mask described above will be included in this chamber.

3.5 *Internal optics structure*

It is planned that the internal off-axis mirror, its support structure, and the optical bench in the SCI will be made of the same material in order to avoid deformation of the optics due to mismatching of the thermal expansion coefficients. The primary candidate for this material is aluminum. Determination of the specification for the mirror quality is ongoing. It is expected that our requirements for the quality of the mirror surface are more relaxed than those for optical coronagraph missions targeting terrestrial planets (Shaklan, Green, & Palacios, 2006) because of the differences in target contrast and the observation wavelength region.

As presented above, key technologies required to realize a coronagraph with spectroscopic capabilities in the MIR for SPICA are being assessed. The indications are that all the major issues, including the binary shaped pupil mask coronagraph for the MIR and the cryogenic adaptive optics, can be resolved.

Acknowledgments

We deeply thank and pay our respects to all the pioneers in this field, especially R. Vanderbei and J. Kasdin. This work is supported by JAXA.

References

- Abe, L., Vannier, M., Petrov, R., Enya, K., & Kataza, H. Characterizing Extra-Solar Planets with Color Differential Astrometry on SPICA, Proc. of SPICA joint European/Japanese Workshop, held 6-8 July, 2009 at Oxford, United Kingdom. Edited by A.M. Heras, B.M. Swinyard, K.G. Isaak, and J.R. Goicoechea. EDP Sciences, 2009, p.02005
- Bordé, P. J., & Traub, W. A., High-Contrast Imaging from Space: Speckle Nulling in a Low-Aberration Regime, *AJ*, 638, 488-498, 2006
- Burrows, A., Sudarsky, D., & Lunine, J. I., Beyond the T Dwarfs: Theoretical Spectra, Colors, and Detectability of the Coolest Brown Dwarfs, *ApJ*, 596, 587-596, 2003
- Charbonneau, D., Brown, T. M., Latham, D. W., & Mayor, M., Detection of Planetary Transits Across a Sun-like Star, *ApJL*, 529, 45-48, 2000
- Deming, D., Seager, S., Richardson, L. J., & Harrington, J., Infrared radiation from an extrasolar planet, *Nature*, 434, 740-743, 2005
- Enya, K., & Abe, L., A Binary Shaped Mask Coronagraph for a Segmented Pupil, *PASJ*, 62, 1407-1411, 2010

- Enya, K., & SPICA Working Group, SPICA infrared coronagraph for the direct observation of exo-planets, *Advances in Space Research*, 45, 979-999, 2010
- Enya, K., Kataza, H., & Bierden, P., A Micro Electrical Mechanical Systems (MEMS)-based Cryogenic Deformable Mirror, *PASP*, 121, 260-265, 2009
- Fukagawa, M., Itoh, Y., & Enya, K. Proc. of SPICA joint European/Japanese Workshop, held 6-8 July, 2009 at Oxford, United Kingdom. Edited by A.M. Heras, B.M. Swinyard, K.G. Isaak, and J.R. Goicoechea. EDP Sciences, 2009, p.02006
- Give'on, A., Kern, B., Shaklan, S., Moody, D. C., & Pueyo, L., Broadband wavefront correction algorithm for high-contrast imaging systems, *Proc. of the SPIE*, 6691, 66910A-66910A-11, 2007
- Haze, K., Enya, K., Abe, L., Tanaka, S., Nakagawa, T., Sato, T., Wakayama, T., & Yamamuro, T., An AO-free coronagraph experiment in vacuum with a binary-shaped pupil mask, *Advances in Space Research*, 43, 181-186, 2009
- Haze, K., Enya, K., Abe, L., Kotani, T., Nakagawa, T., Sato, T., & Yamamuro, T., Multi-color coronagraph experiment in a vacuum testbed with a binary shaped pupil mask, *PASJ*, submitted
- Honda, M., Inoue, A. K., Fukagawa, M., Oka, A., Nakamoto, T., Ishii, M., Terada, H., Takato, N., Kawakita, H., Okamoto, Y. K., Shibai, H., Tamura, M., Kudo, T., & Itoh, Y. *ApJ*, 690, L110-L113, 2009
- Kalas, P., Graham, J. R., Chiang, E., Fitzgerald, M. P., Clampin, M., Kite, E. S., Stapelfeldt, K., Marois, C., & Krist, J., Optical Images of an Exosolar Planet 25 Light-Years from Earth, *Science*, 322, 1345-1348, 2008
- Kasdin, N. J., Vanderbei, R. J., Littman, M. G. & Spergel, D. N., Optimal one-dimensional apodizations and shaped pupils for planet finding coronagraphy, *Applied Optics*, 44, 1117-1128, 2005b
- Kotani, T., Enya, K., Nakagawa, T., Abe, L., Miyata, T., Sako, S., Nakamura, T., Haze, K., Higuchi, & S., Tange, Y., A Wavefront Correction System for the SPICA Coronagraph Instrument, *Proc. of Pathways Towards Habitable Planets*, ASP Conference Series, Vol. 430, pp. 477-479, 2010. Eds. Vincent Coudé du Foresto, Dawn M. Gelino, and Ignasi Ribas, 14-18 September, 2009, Barcelona, Spain. Print ISBN: 978-1-58381-740-7
- Malbet, F., Yu, J. W., & Shao, M. High-Dynamic-Range Imaging Using a Deformable Mirror for Space Coronagraphy, *PASP*, 107, 386-398, 1995
- Marois, C., Macintosh, B., Barman, T., Zuckerman, B., Song, I., Patience, J., Lafrenière, D., & Doyon, R., Direct Imaging of Multiple Planets Orbiting the Star HR 8799, *Science*, 322, 1348-1352, 2008
- Matsuo, T., Fukagawa, M., Kotani, T., Itoh, Y., Tamura, M., Nakagawa, T., Enya, K., & SCI team, Direct Detection and Spectral Characterization of Outer Exoplanets with SPICA Coronagraph Instrument(SCI). *Advances in Space Research*, in press
- Mayor, M., & Queloz, D., A Jupiter-Mass Companion to a Solar-Type Star, *Nature*, 378, 355-359, 1995
- Nakagawa, T., & SPICA team, The next generation space infrared astronomy

- mission SPICA, Proc. of SPIE, 2010, in press
- Narita, N., Yamashita, T., Enya, K., & SCI team, Study of transiting exoplanets with the SCI and instruments of SPICA, *Advances in Space Research*, submitted (TBC later)
- Okaji, M., & Yamada, N., Precise Thermal Expansion Measurements of Single Crystal Silicon with an Interferometric Dilatometer, *Bulletin of NRLM*, 48, 251-258, 1999
- Shaklan, S. B., Green, J. J., Palacios, D. M., The terrestrial planet finder coronagraph optical surface requirements, *Proc. of SPIE*, 6265, pp. 62651I, 2006
- Swain, M. R., Tinetti, G., Vasisht, G., Deroo, P., Griffith, C., Bouwman, J., Chen, Pin, Yung, Y., Burrows, A., Brown, L. R., Matthews, J., Rowe, J. F., Kuschnig, R., & Angerhausen, D., Water, Methane, and Carbon Dioxide Present in the Dayside Spectrum of the Exoplanet HD 209458b, *ApJ*, 704, 1616-1621, 2009
- Tanaka, S., Enya, K., Abe, L., Nakagawa, T., % Kataza, H., Binary-Shaped Pupil Coronagraphs for High-Contrast Imaging Using a Space Telescope with Central Obstructions, *PASJ*, 58, 627-639, 2006
- Tamura, M., Takami, M., Enya, K., Ootsubo, T., Fukagawa, M., Honda, M., Okamoto, Y. K., Sako, S., Yamashita, T., Hasegawa, S., Kataza, H., Doi, Y., Matsuhara, H., & Nakagawa, T., Proc. of SPICA joint European/Japanese Workshop, held 6-8 July, 2009 at Oxford, United Kingdom. Edited by A.M. Heras, B.M. Swinyard, K.G. Isaak, and J.R. Goicoechea. EDP Sciences, 2009, p.02001
- Takami, M., Tamura, M., Enya, K., Ootsubo, T., Fukagawa, M., Honda, M., Okamoto, Y., Sako, S., Yamashita, T., Hasegawa, S., Kataza, H., Matsuhara, H., Nakagawa, T., Goicoechea, J. R., Isaak, K., & Swinyard, B., Studies of exoplanets and solar systems with SPICA, *Advances in Space Research*, 45, 1000-1006, 2010
- Tinetti, G., Vidal-Madjar, A., Liang, M.-C., Beaulieu, J.-P., Yung, Y., Carey, S., Barber, R. J., Tennyson, J., Ribas, I., Allard, N., Ballester, G. E., Sing, D. K., & Selsis, F., Water vapour in the atmosphere of a transiting extrasolar planet, *Nature*, 448, 169-171, 2007
- Trauger, J. T., Traub, W. A., A laboratory demonstration of the capability to image an Earth-like extrasolar planet, *Nature*, 446, , 771-773, 2007
- Vanderbei, R. J., Kasdin, N. J. & Spergel, D. N., Checkerboard-Mask Coronagraphs for High-Contrast Imaging, *ApJ*, 615, 555-561, 2004
- Vanderbei, R. J., LOQO: an interior point code for quadratic programming, *Optimization methods and software*, 11, 451-484, 1999

Table 1
Specification for the SCI

Wavelength (λ)*	Core wavelength $\lambda = 3.5\text{-}27\mu\text{m}$ Short wavelength channel: $\lambda = 3.5\text{-}5\mu\text{m}$ Long wavelength channel: $\lambda \geq 5\mu\text{m}$
Coronagraph method	Binary shaped pupil mask
Observation mode	Coronagraphic imaging Coronagraphic spectroscopy Non-coronagraphic imaging Non-coronagraphic spectroscopy
contrast	10^{-6} @PSF
Inner working angle (IWA)	$3.3\lambda/D$ **
Outer working angle (OWA)	$16\lambda/D$
Filter	Band-pass filters for each channel
Detector	a $1\text{K} \times 1\text{K}$ Si:As array for the long wavelength channel a $1\text{K} \times 1\text{K}$ InSb array for the short wavelength channel
FoV	High-contrast coronagraphic FoV: $16\lambda/D$ (FoV of $1' \times 1'$ is available but high-contrast is not guaranteed out of $16\lambda/D$)
Spectral resolution	~ 20 and ~ 200 (realized by transmissive dispersion devices, e.g. grisms)

* At $\lambda < 3.5\mu\text{m}$, high contrast imaging is not guaranteed, but the instrument has sensitivity through the InSb detector.

* D is telescope aperture diameter.

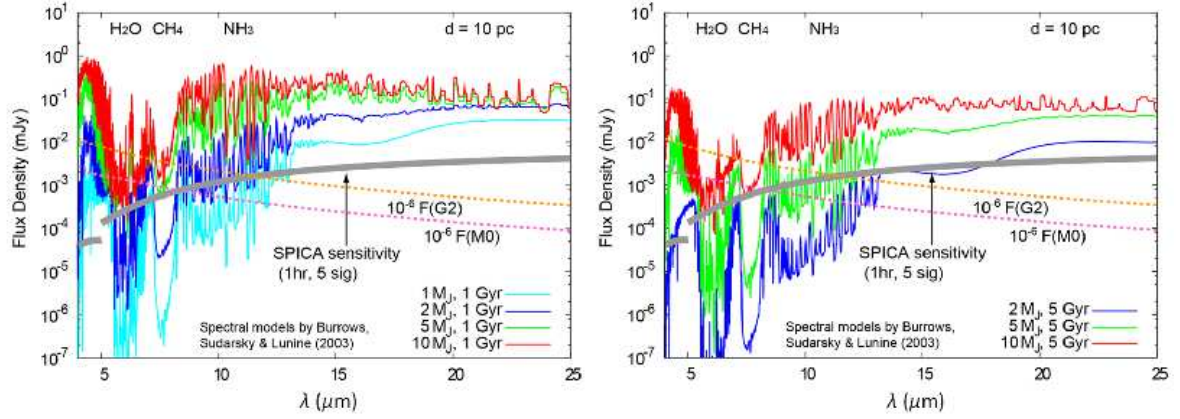


Fig. 1. Calculated SEDs of 1 Gyrs (left) and 5 Gyrs (right) old Jovian planets with various masses presented as Fig. 13 in Burrows, Sudarsky, & Lunine (2003), and properties relating to SPICA observations. 10pc is assumed as the distance to the planetary system. The gray solid curve shows the sensitivity limit of imaging with SPICA. The orange and purple dashed lines show the scaled SEDs of G2 and M0 type stars, respectively. These figures are from Fukagawa, Itoh, & Enya (2009).

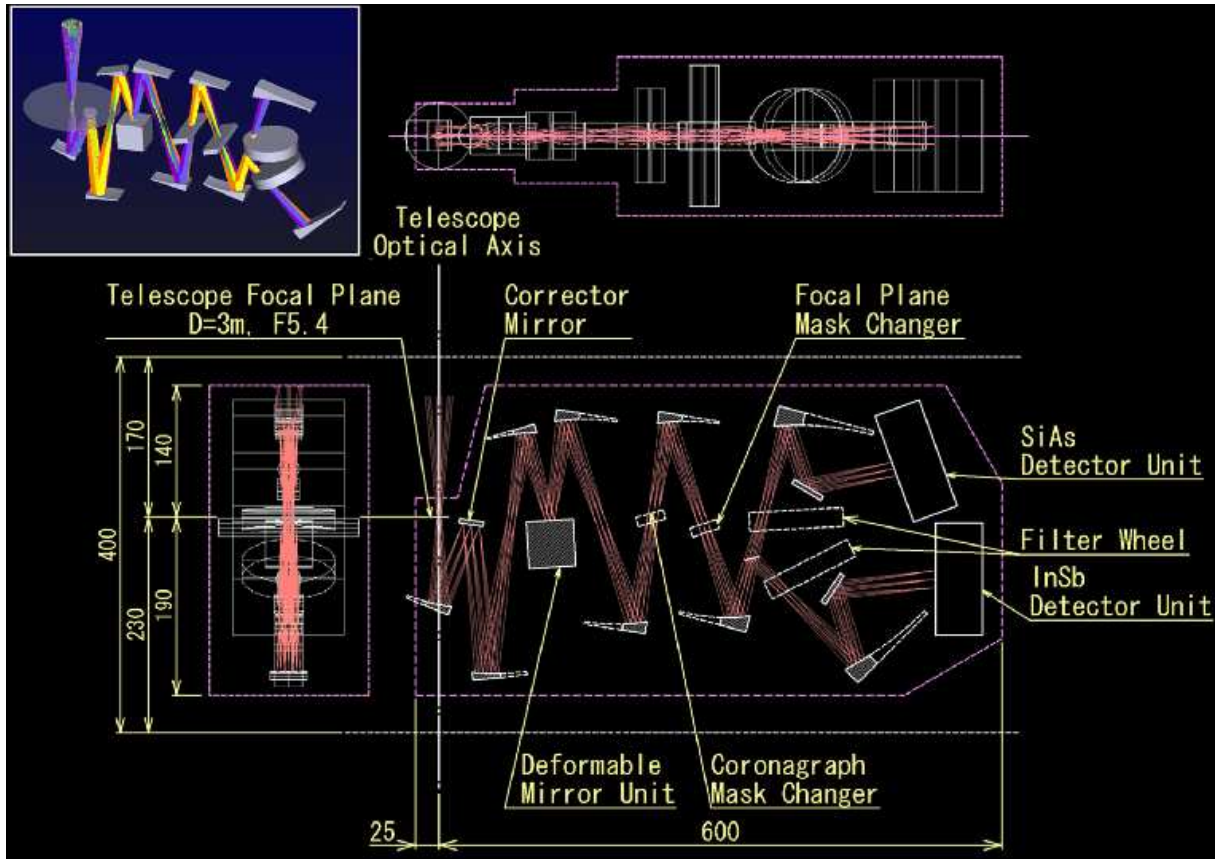


Fig. 2. Overview of the optical design of the SCI.

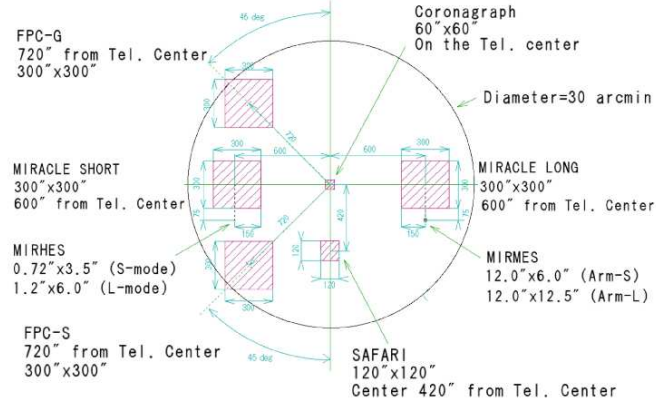


Fig. 3. Current design of the distribution of the FoV for the SPICA instruments.

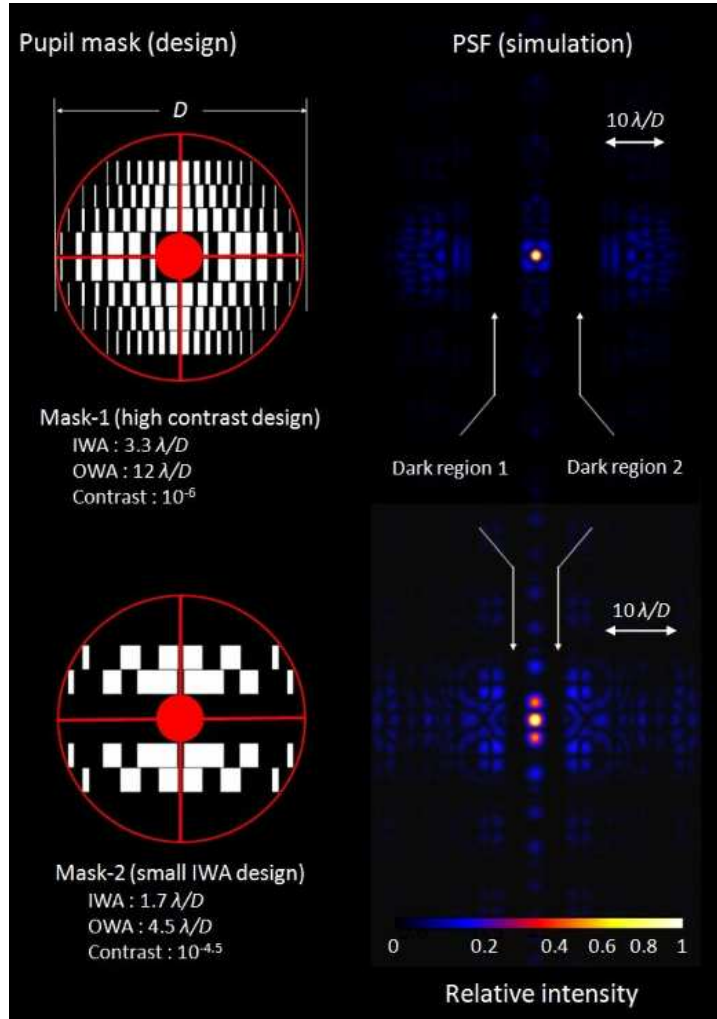


Fig. 4. Design of a multi-barcode 1D coronagraph for the SPICA pupil. Top and bottom panels show current baseline and an optional design, respectively. The mask design (left) and the simulated PSF using this pupil (right). Transmissivity of the mask is 1 and 0 at white and black area, respectively.

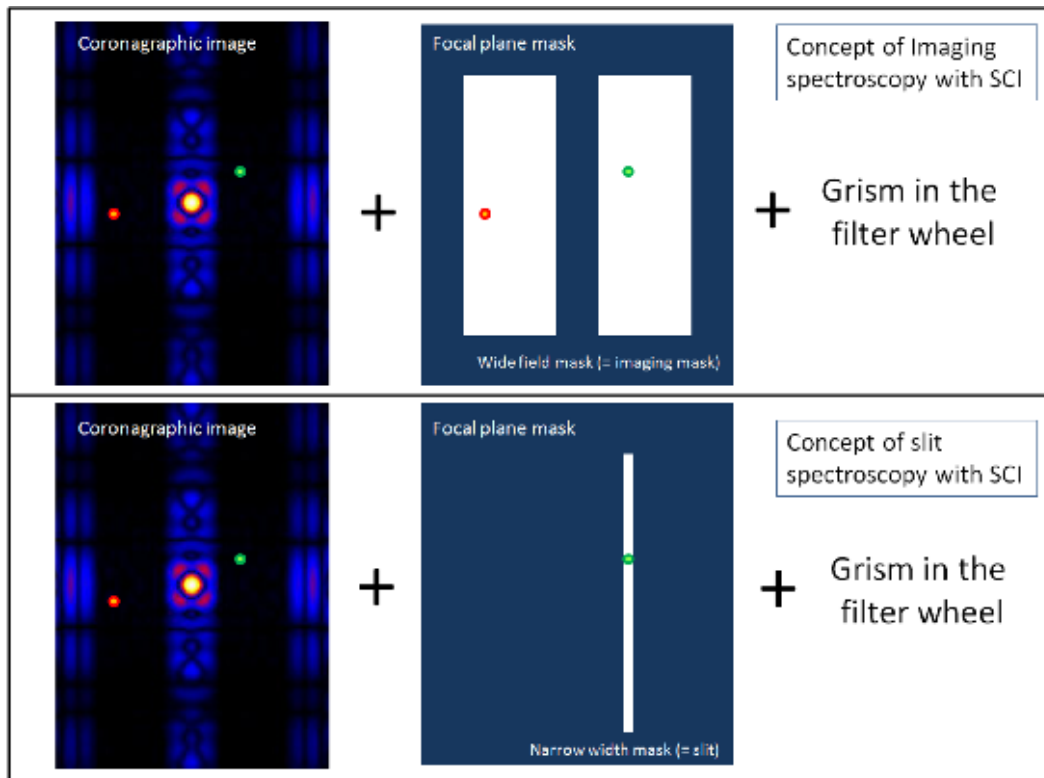


Fig. 5. Spectroscopy working together with coronagraphy in the SCI.

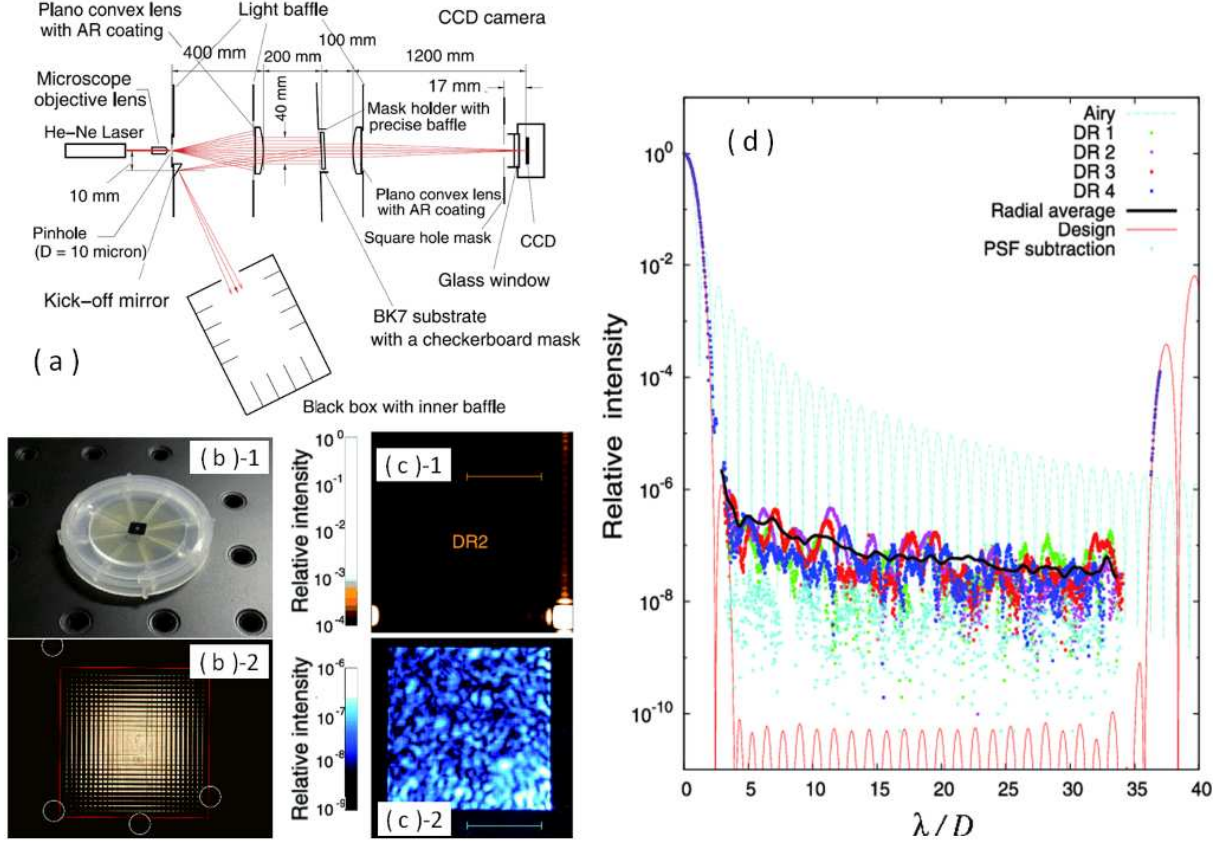


Fig. 6. (a): Configuration used in demonstrating the operation of a binary shaped pupil mask. (b): Checkerboard mask manufactured on a glass substrate by nano-fabrication technology using electron beam lithography and a lift-off process. Top and bottom panels show whole of the device, and microscopic image, respectively. This mask is designed to produce four dark region of square shape, DR1-DR4, around the core of the PSF. (c): Experimental PSF (top) and high sensitivity image of a dark region, DR2, of the PSF (bottom). (d): The observed and theoretical coronagraphic profiles as well as the theoretical Airy profile. Each profile is normalized to the peak intensity in each image.

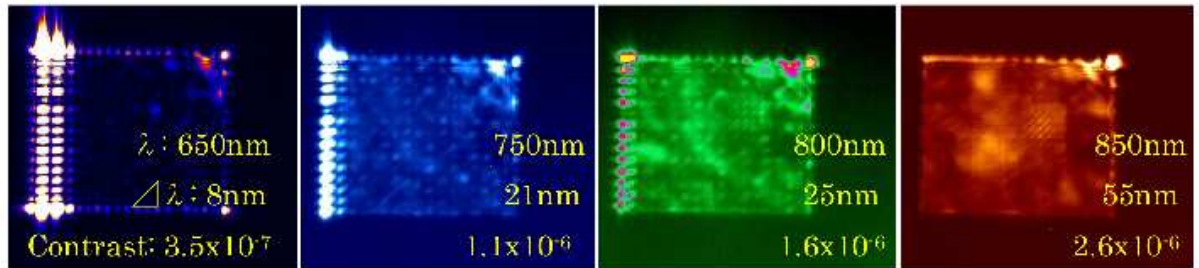


Fig. 7. Results of a multi-color/broadband experiment using a checkerboard mask. Only images of the dark region are shown. Ghosting caused by the lens puts a practical limit on the contrast at longer wavelengths.



Fig. 8. Left: a free standing checkerboard mask made of a thin copper plate installed in the test setup using a visible laser in air. Middle and right: microscope pictures of the free standing checkerboard mask made of thin copper plate.

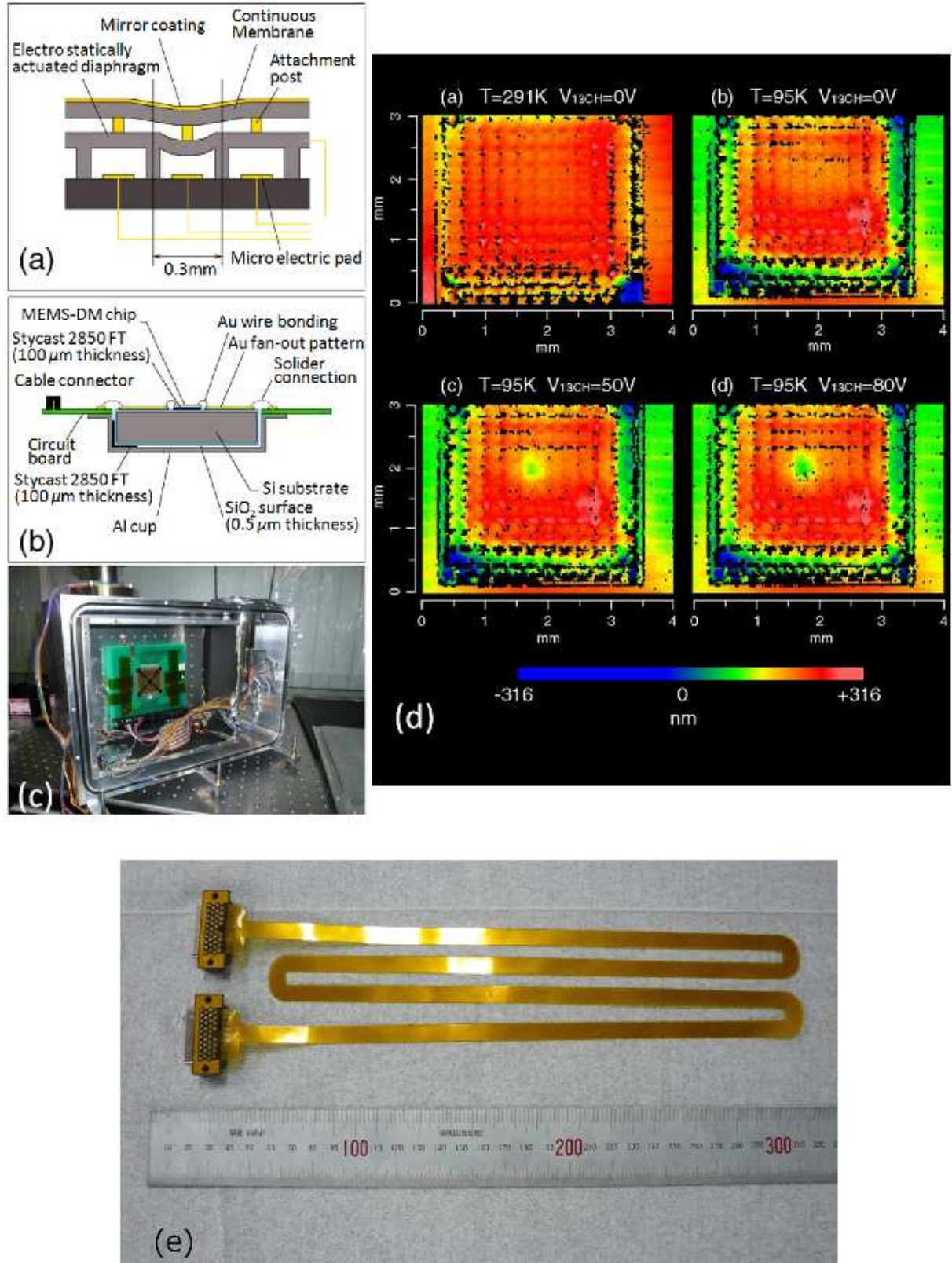


Fig. 9. (a)-(c): schematic views and a photograph of the prototype cryogenic DM unit. (d): results of a demonstration of the prototype cryogenic DM. (e): A sample of the film print cable.

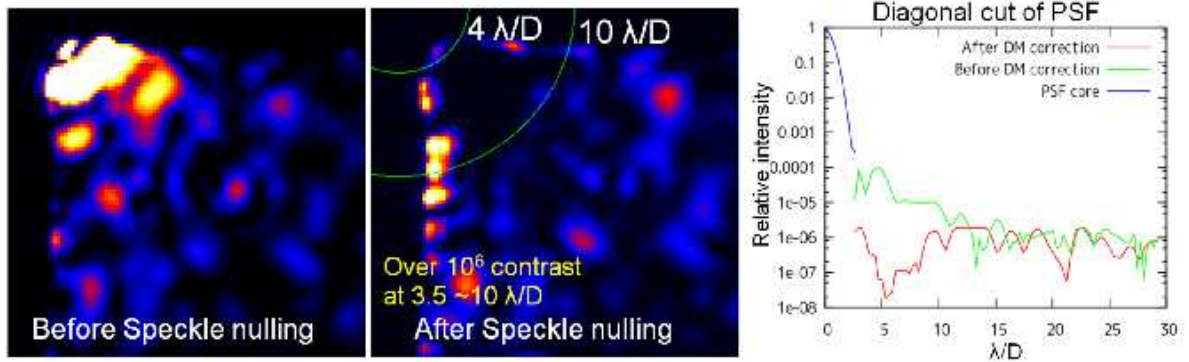


Fig. 10. Results of the speckle nulling experiment. Left and middle: images of a dark region of the PSF obtained with a square hole mask, before and after speckle nulling, respectively. Right: Diagonal cut through the PSF.